

# Influence of cathode functional layer composition on electrochemical performance of solid oxide fuel cells

Antônio de Pádua Lima Fernandes<sup>1</sup> · Eric Marsalha Garcia<sup>2</sup> ·  
Rubens Moreira de Almeida<sup>1</sup> · Hosane Aparecida Taroco<sup>2</sup> ·  
Edyth Priscilla Campos Silva<sup>1</sup> · Rosana Zacarias Domingues<sup>1</sup> · Tulio Matencio<sup>1</sup>

Received: 30 September 2015 / Revised: 27 April 2016 / Accepted: 8 May 2016 / Published online: 20 May 2016  
© Springer-Verlag Berlin Heidelberg 2016

**Abstract** In this work, anode-supported solid oxide fuel cells (SOFC) were tested with a yttria-stabilized zirconia (YSZ) (8 mol%  $Y_2O_3$ - $ZrO_2$ )/gadolinium-doped ceria (GDC) ( $Ce_{0.9}Gd_{0.1}O_{1.95}$ ) bilayer electrolyte and two lanthanum strontium cobalt ferrite (LSCF) composition as functional cathode layer:  $La_{0.6}Sr_{0.4}Co_{0.8}Fe_{0.2}O_{3-\delta}$  (LSCF 1) and  $La_{0.60}Sr_{0.40}Co_{0.2}Fe_{0.8}O_{3-\delta}$  (LSCF 2). The functional cathode layers were made of 50 % (w/w) LSCF and 50 % (w/w) GDC. Microstructural characterization was performed by scanning electron microscopy and X-ray diffraction. Electrochemical impedance spectroscopy (EIS) and power measurements were performed under oxygen and hydrogen atmospheres. The microscopy studies showed that the LSCF 2 functional layer is more uniform and adherent to the electrolyte and the cathode collector than the LSCF 1 functional layer, which has cracks, chips, and lower adhesion. The use of the LSCF 2 layer allowed an approximately 25-fold reduction in ohmic resistance ( $0.06 \Omega \text{ cm}^{-2}$ ) compared with the LSCF 1 layer ( $1.5 \Omega \text{ cm}^{-2}$ ). The power measurements showed a considerable increase in the power cell using LSCF 2 (approximately  $420 \text{ mW cm}^{-2}$ ) compared with the power cell using LSCF 1 (approximately  $180 \text{ mW cm}^{-2}$ ).

**Keywords** SOFC · LSCF · Interface · Electrochemical performance · Cathode · Functional layer

✉ Tulio Matencio  
tmatencio@ufmg.br

<sup>1</sup> Department of Chemistry, Federal University of Minas Gerais (UFMG), Belo Horizonte, Brazil

<sup>2</sup> DECEB, Federal University of São João del-Rei (UFSJ), Sete Lagoas, Brazil

## Introduction

Solid oxide fuel cells (SOFC) are devices that transform the chemical energy of a fuel directly into electricity, typically with a good energy efficiency of around 75 % [1–4]. The use of hydrogen as a fuel implies the absence of  $CO_2$  emissions and other pollutants, and fuel cells are therefore considered a clean energy technology [1–4]. SOFCs are typically composed of solid anode and cathode electrodes separated by a dense electrolyte layer composed commonly by an ion conductive ceramic oxide such as  $Y_2O_3$  stabilized with  $ZrO_2$  (YSZ) or Ce and Ga oxide GDC [4]. The use of these materials requires operating temperatures above  $800 \text{ }^\circ\text{C}$  in order to provide the desired cell power. Reducing this operating temperature is important in enabling the use of lower cost materials, to reduce occurrence of undesired reactions, to reduce the time required for device initialization, and to decrease the thermal stress between fuel cell components [2]. However, the operation of SOFCs at lower temperatures increases the role of electrode polarization in relation to ionic transport, which is a great limiting factor for overall cell performance. Moreover, the decrease in operating temperature increases the activation energy for  $O_2$  reducing in cathode, making this process the reaction determinant step for SOFC operation. [3, 4]. Thus, to minimize the ohmic loss in SOFC operation, many papers are devoted to research new cathode materials that operate efficiently at lower temperatures [6, 7]. The cathode must have an appropriate chemical composition to obtain the ideal microstructure, particularly in the cathode-electrolyte interface [8–11]. The cobalt-containing oxide phases with  $ABO_3$  perovskite structure have great electrochemical activity under the SOFC cathodic conditions [4]. In this sense, the perovskite oxide  $La_{(1-y)}Sr_yCo_{(1-x)}Fe_xO_{3-\delta}$  (LSCF) have attracted great attention due to their high mixed electronic–ionic conduction, becoming a promising candidate to cathode for

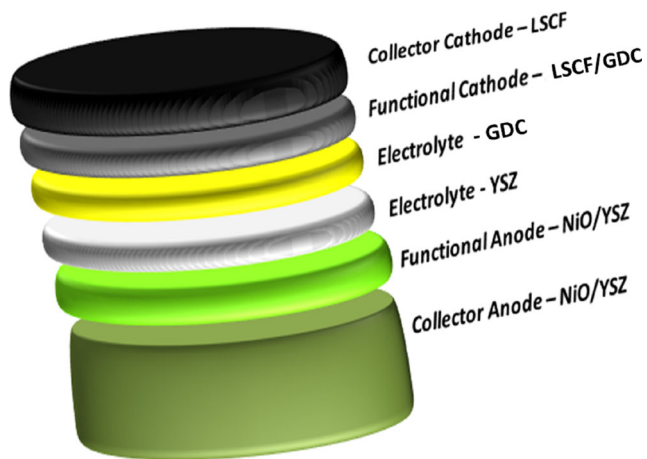


Fig. 1 Schematization of fuel cell layout used in this work

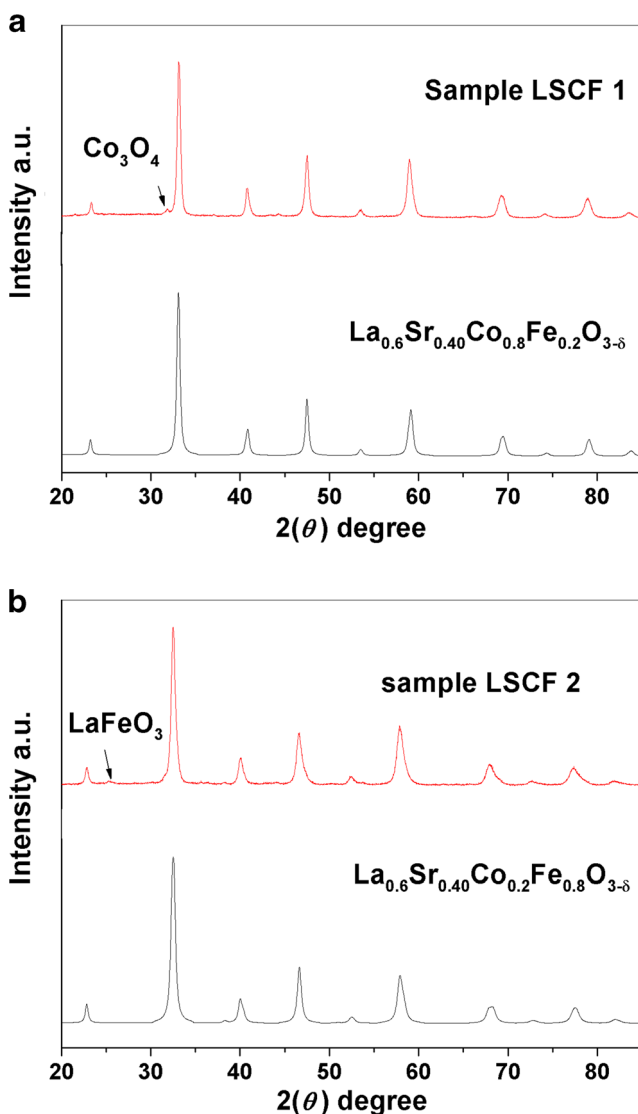
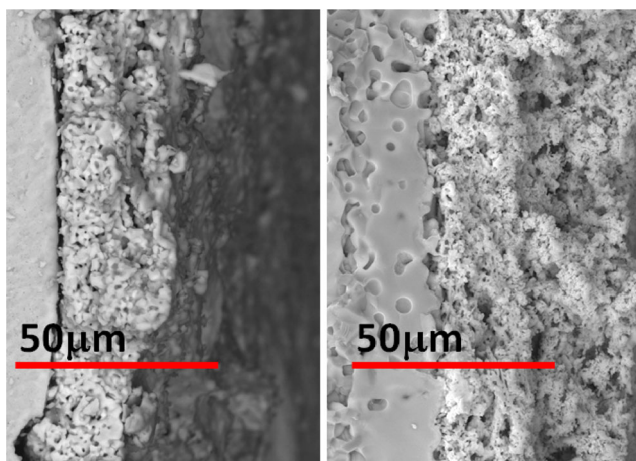


Fig. 2 X-ray diffraction patterns of LSCF 1 (a) and LSCF 2 (b) powders

intermediate temperature solid oxide fuel cells (IT-SOFC) [5]. Moreover, it is reported that the electrical conductivity of the  $\text{La}_{0.6}\text{Sr}_{0.4}\text{Co}_{0.2}\text{Fe}_{0.8}\text{O}_3$  reaches  $300 \text{ S cm}^{-1}$  at  $600 \text{ }^\circ\text{C}$  in  $\text{O}_2$  atmosphere [5]. One alternative that has been widely used to improve LSCF performance is the inclusion of a functional layer between the cathode and electrolyte with reduced thickness and a different microstructure compared to the cathode current collector [12, 13]. The deposition of a functional layer can be achieved using various techniques, which are selected according to the desired layer thickness [14, 15]. In the literature, we find work by Hildenbrand and coworkers describing the improvement obtained in a  $\text{La}_2\text{NiO}_{4+\delta}$  cathode after adding a  $\text{La}_{0.6}\text{Sr}_{0.4}\text{Co}_{0.2}\text{Fe}_{0.8}\text{O}_{3-\delta}$  functional layer deposited by pulsed laser [16, 17]. Dumaisnil and coworkers recently conducted a study on a thin layer (700 nm thick) of LSCF deposited between a  $\text{Ce}_{0.9}\text{Gd}_{0.1}\text{O}_{2-\delta}$  electrolyte and LSCF cathode [18]. Compared with the  $\text{La}_{1-x}\text{Sr}_x\text{MnO}_{3-\delta}$  (LSM), the most commonly used material for cathodes, the  $\text{La}_{(1-x)}\text{Sr}_x\text{Co}_{(1-y)}\text{Fe}_y\text{O}_{3-\delta}$ , presents itself as a potential candidate for use as a collector and functional cathode because it has both electronic and ionic conductivity [19]. Generally, ionic and electronic conductivity and catalytic activity increase when  $x$  increases and  $y$  decreases, whereas chemical compatibility with the electrolyte and the thermal expansion coefficient have the opposite trend [20, 21]. Although the electronic LSCF conductivity is high, the conductivity of oxygen ions is very low (approximately  $0.01 \text{ S cm}^{-1}$  at  $700 \text{ }^\circ\text{C}$ ) [22]. Conversely, the ionic conductivity of the most common electrolyte (8YSZ) is approximately  $0.02 \text{ S cm}^{-1}$  [23]. This difference becomes more significant at lower temperatures. Thus, if LSCF is used as cathode material, the electrochemical reaction is limited to the region of the cathode/electrolyte interface, which leads to an increase in the cathode polarization resistance. To increase the ionic conductivity of the cathode, an interesting alternative would be to add a conductor of oxygen ions, such as ceria doped with gadolinium (GDC), into the functional layer and change the LSCF composition used in this layer [24, 25].

In this work, anode-supported solid oxide fuel cells containing a cathode functional layer of LSCF will be tested using two different compositions,  $\text{La}_{0.6}\text{Sr}_{0.4}\text{Co}_{0.8}\text{Fe}_{0.2}\text{O}_{3-\delta}$  (LSCF 1) and  $\text{La}_{0.6}\text{Sr}_{0.4}\text{Co}_{0.2}\text{Fe}_{0.8}\text{O}_{3-\delta}$  (LSCF 2). The cathode functional layers were made of 50 % (w/w) LSCF and 50 % (w/w) GDC. The functional layers were deposited by screen printing and reached an average thickness of  $10 \mu\text{m}$ . A screen printing method was chosen because it has a relatively low cost, is easy to operate, is highly reproducible, and can be used on a large scale. To investigate the influence of LSCF composition, we used button cells supported by a nickel oxide-



**Fig. 3** Scanning electron microscopy of interface between GDC and the LSCF 1 functional layer (a) and LSCF 2 functional layer (b)

Ytria-stabilized zirconia (NiO-YSZ) anode covered with a 10- $\mu\text{m}$  layer of YSZ electrolyte and 10- $\mu\text{m}$  layer of GDC electrolyte to prevent a reaction between zirconia YSZ and lanthanum strontium or LSCF [25].

### Methodology

For this study, NiO-YSZ anode-supported fuel cells were prepared, and two electrolyte layers were deposited on the support, one with YSZ (with a thickness of 10  $\mu\text{m}$ ) and the other with CGD (with a thickness of 10  $\mu\text{m}$ ). Functional and collector cathodes were then deposited. Figure 1 shows the details of the different layers forming the fuel cell.

### Anode and electrolyte preparations

The anode was prepared using a tape casting technique [26]. Pellets were produced with a 2.0-cm diameter and were 1.0 mm thick. These pellets were sintered at 1200  $^{\circ}\text{C}$ . The electrolyte YSZ was deposited by spray coating using a suspension prepared from synthetic powder Tosoh (Japan); 12 overlapping layers were used to obtain the desired thickness. The deposited film was then sintered at 1500  $^{\circ}\text{C}$  [27]. After sintering, a 10- $\mu\text{m}$  GDC layer was deposited using the same deposition and sintering procedures and parameters as for the first electrolyte. The GDC suspension used was also prepared from commercial powders (Fuel Cell Materials). To ensure a better densification, 1.0 % of Zn powder was added to GDC. The procedure used in this addition is detailed in the literature. [28].

### LSCF preparation

The two LSCF powder compositions were synthesized through a citrate route using nitrates of the metals as starting

components in molar proportions according to each composition. The suspensions of LSCF 1 and LSCF 2 used for the production of the functional layer were prepared from a mixture of 50 % by mass of LSCF powder and 20 % of commercial GDC powder homogenized with ethyl cellulose, alpha terpineol, and isopropanol using a ball mill for 5 h. The functional cathode films were then deposited by screen printing on the Ni-YSZ anode support containing YSZ and GDC layers

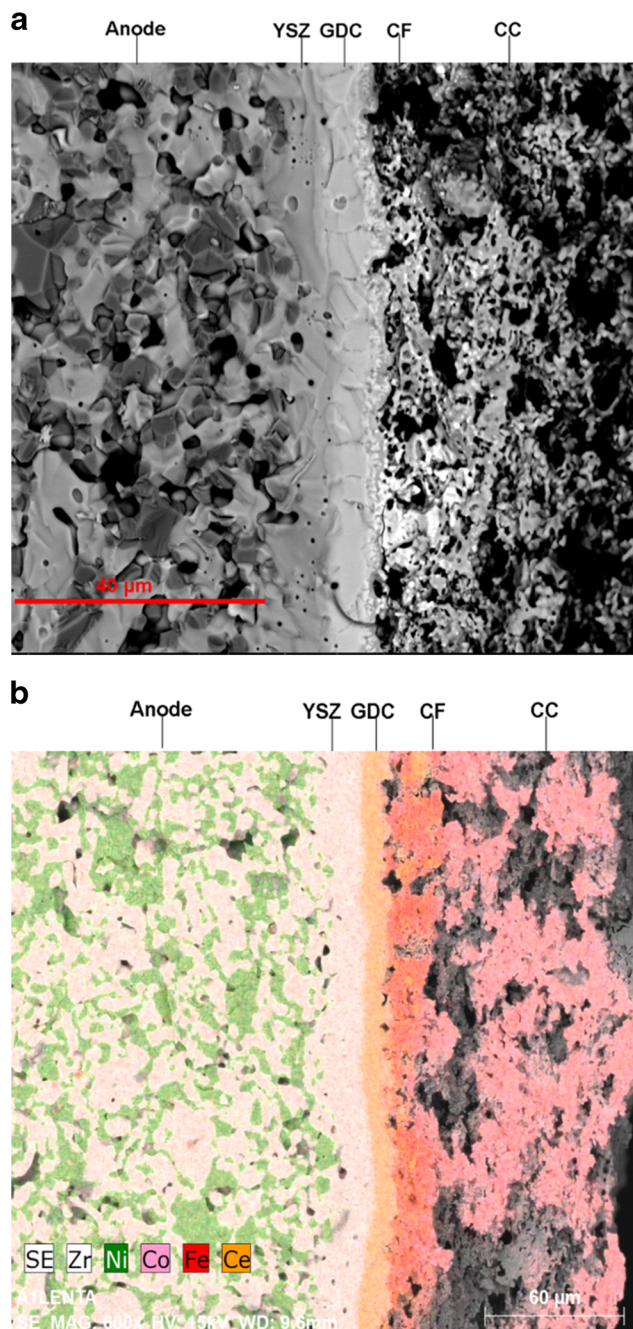


**Fig. 4** (a) Scanning electron microscopy of the optimized fuel cell (b) EDS image of the LSCF 2 functional layer (CF) and the LSCF 1 collector layer (CC)

using a pressure of 2.0 bar and squeegee speed of  $70 \text{ mm sec}^{-1}$ . Four layers were deposited to obtain the desired film thickness. In all of the studied fuel cells, LSCF 1 powder was used to produce the cathode collector. The suspension used for the LSCF 1 layer collector was produced from 60 % LSCF 1 by mass homogenized with ethyl cellulose, alpha terpineol, and isopropanol using a ball mill for 4 h. The cathode collector films were deposited by screen printing using the same parameters as for the functional layer except that the desired thickness was obtained with the deposition of 20 layers. The area of the cathodes was  $0.75 \text{ cm}^2$ .

### Scanning electron microscopy

The cathode surface films, the interface between cathode and electrolyte layers, and the cathode porosity films were analyzed by scanning electron microscopy (SEM) images collected using a QUANTA Microscope Model 200 RL. Energy dispersive scanning (EDS) images were used to verify the densification efficiency of the GDC electrolyte and thus precluded the migration of strontium into the YSZ electrolyte.

### Electrochemical measurements

All electrical tests were made using a NorECs<sup>®</sup> cell electrical measurement. The impedance and electrical measurements were performed using a PGSTAT AUTOLAB 302 with a FRA impedance module and FRA and GPES software. The electrochemical impedance spectroscopy measurements were performed in the frequency range from  $10^5$  to  $10^{-2}$  Hz with an AC amplitude of 10 mV. All experimental measurements were performed between 650 and 850 °C at a flow rate of  $85 \text{ ml min}^{-1}$  for  $\text{H}_2$  at the anode and  $120 \text{ ml min}^{-1}$  for  $\text{O}_2$  at

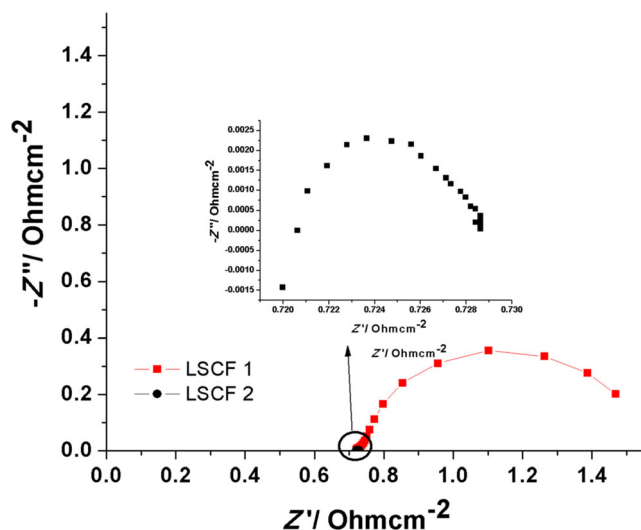


**Fig. 5** Nyquist plot for LSCF 1 and LSCF 2 functional layers

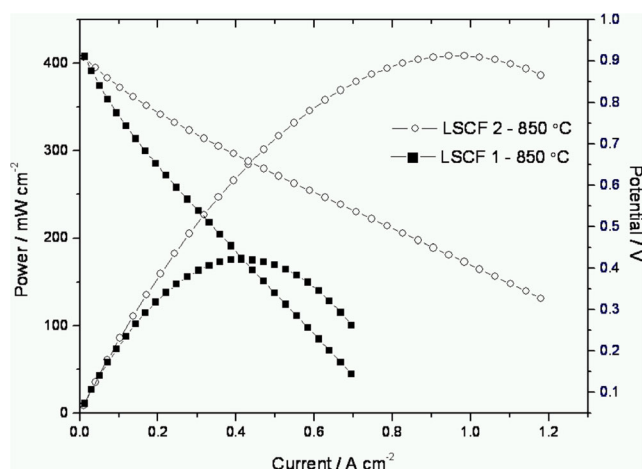


**Fig. 6** Power density at 850 °C of fuel cells with LSCF 1 and LSCF 2 functional layers

the cathode.  $\text{N}_2$  at a flow rate of  $50 \text{ ml min}^{-1}$  was used as the  $\text{H}_2$  carrier.

## Result and discussion

### LSCF 1 and LSCF 2 powders characterization

LSCF powders were characterized by X-ray diffraction. Diffraction patterns, shown in Fig. 2, show that both LSCF powders were satisfactorily obtained and that the route chosen is suitable for synthesis. Both starting powders (LSCF 1 and 2) are not single-phase. The phase impurities may substantially affect electrochemical properties and stability. Thus, the Rietveld refinement was made using the Fullprof<sup>®</sup> software. The LSCF 1 has 94 % of  $\text{La}_{0.6}\text{Sr}_{0.4}\text{Co}_{0.8}\text{Fe}_{0.2}\text{O}_{3-\delta}$  and 6 % of  $\text{Co}_3\text{O}_4$ . By the other hand, the LSCF 2 has around 99 % of  $\text{La}_{0.6}\text{Sr}_{0.4}\text{Co}_{0.2}\text{Fe}_{0.8}\text{O}_{3-\delta}$  and 1 % of  $\text{LaFeO}_3$ .

Figure 3 shows the interface between GDC and the LSCF 1 and LSCF 2 functional layer. The LSCF 1 layer has few pores, which creates a barrier to oxygen diffusion. It is also possible to see that the adhesion of this layer to the electrolyte is unsatisfactory, causing detachment of the functional layer and thus increasing the cell polarization resistance. The distinct microstructure and adhesion can be explained by thermal expansion coefficient (TEC) in each LSCF composition [29]. The partial substitution of Co by Fe promotes a decrease in the TEC value. For  $\text{La}_{0.6}\text{Sr}_{0.4}\text{Co}_{0.8}\text{Fe}_{0.2}\text{O}_{3-\delta}$  (LSCF 1), the value of TEC is  $15.97 \times 10^{-6} \text{ K}^{-1}$  and for  $\text{La}_{0.6}\text{Sr}_{0.4}\text{Co}_{0.2}\text{Fe}_{0.8}\text{O}_{3-\delta}$  (LSCF 2) the TEC is  $13.19 \times 10^{-6} \text{ K}^{-1}$  [30]. Considering that the TEC for CGD is around  $\sim 12 \times 10^{-6} \text{ K}^{-1}$ , the composition LSCF 2 is more compatible, which results in a better adhesion [31].

The LSCF 2 layer has a porosity greater than the LSCF 1 layer, favoring the diffusion of oxygen, and the change in the

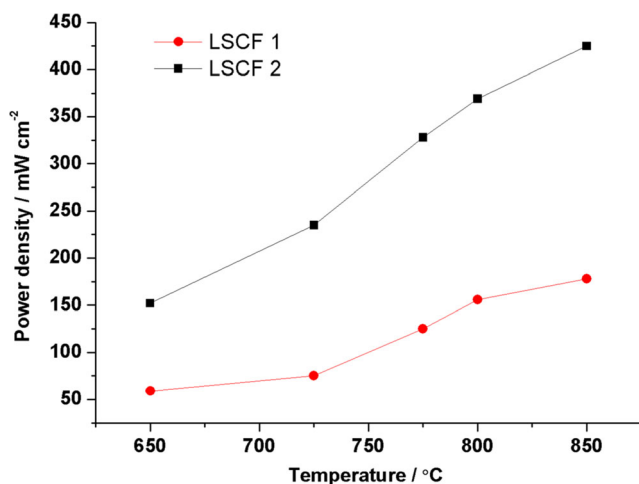


**Fig. 7** Power density measurements versus temperature of fuel cells with LSCF 1 and LSCF 2 functional layers

composition leads to better adhesion of the functional layer, decreasing the resistance polarization (Fig. 3).

Figure 4a shows a fuel cell produced with a functional LSCF 2 cathode 2 and a collector LSCF 1 cathode (optimized cell). The picture clearly shows all layers constituting the fuel cell. All layers exhibit good adhesion at the interfaces, and there is a considerable difference in porosity between the functional layers and the cathode collector without any deficiency in the adhesion between them. Figure 4b shows the chemical map (EDS image) of an entire fuel cell, demonstrating that there is no migration of elements from the cathode toward the YSZ electrolyte, which could result in the formation of insulating layers. This fact proves the effectiveness of the zinc presence to the CGG densification.

### Electrochemical measurements

The electrochemical performance of the fuel cells was tested and compared. From electrochemical impedance spectroscopy (EIS) measurements, it was possible to evaluate the polarization resistance alteration due to the change in composition of the cathode functional layer. Figure 5 shows EIS measurements at 850 °C carried out in the open circuit potential of the fuel cell produced with LSCF 1 and LSCF 2 functional layers. In both cases, the best electrical circuit adjusted for experimental result was  $LR_e(R_pQ)$ , where  $L$  is the inductor element,  $Q$  is the constant phase element,  $R_e$  is the ohmic resistance of electrolyte, and  $R_p$  is the polarization resistance of anode and cathode reactions [32–34]. The ohmic resistance associated with the electrolyte ionic conductivity is of the same order (approximately  $0.72 \Omega \text{ cm}^{-2}$ ) for both samples. For the LSCF 1 and LSCF 2 functional layers, the polarization resistance was approximately 1.5 and  $0.06 \Omega \cdot \text{cm}^{-2}$ , respectively. The same conditions were adopted in two experiments, varying only the composition of the functional layer. Thus, even that the  $R_p$  comprises the anode, cathode, and electrolyte

contributions, any change in the resistance polarization is mainly related to the charge transfer of  $\text{O}_2$  reduction because only cathode composition was changed. The greatest  $R_p$  obtained for LSCF 1 must be related to their low adhesion to electrolyte (Fig. 3a).

The improved performance after the change in the composition of the functional cathode is quite clear. The polarization resistance was reduced by a factor of 25, which proves that this configuration leads to a functional layer microstructure that allows for better diffusion of oxygen and increased grip on the electrolyte, favoring an increase of three phase boundary regions (TPB).

Figure 6 shows the power density measurement diagram obtained at 850 °C for the studied fuel cells. The cell produced with the LSCF 2 functional layer has a maximum power density of approximately  $410 \text{ mW cm}^{-2}$  whereas the maximum power density of the other fuel cell was approximately  $180 \text{ mW cm}^{-2}$ .

Figure 7 shows power density measurements versus temperature of the fuel cells. At all temperatures, measurement of the fuel cell with LSCF 2 functional cathode layer clearly confirms that it has the best performance. The LSCF 1 fuel cell had a maximum output power density of approximately  $180 \text{ mW cm}^{-2}$  at 850 °C whereas the other fuel cell at this same temperature had a maximum output power density of approximately  $420 \text{ mW cm}^{-2}$ .

### Conclusions

The influence of the change in the composition of the material used as a functional cathode of a SOFC in their electrochemical and microstructural properties was investigated. The change in LSCF powder composition modifies the porosity of the functional layer and improves its adhesion to the CGD electrolyte. The electrochemical cell performance improved significantly, with a decrease by a factor of approximately 25 in the cell polarization resistance, which can be attributed to the fact that the modified cell microstructure in the functional layer allows for better diffusion of oxygen and increases the grip of the electrolyte favoring an increase in the regions of TPB. An improvement in power density performance of the fuel cell was observed over the whole temperature range studied.

**Acknowledgments** The authors acknowledge UFMG (Pró-Reitoria de Pesquisa), CNPq (project: 407186/2013-1 and 472767/2013-5), CAPES, FAPEMIG, and CEMIG for financial support and the Center of Microscopy at the Universidade Federal de Minas Gerais for providing the equipment and technical support for experiments involving electron microscopy.

## References

- Zhang X, Chan SH, Li G, Ho HK, Li J, Feng Z (2010) A review of integration strategies for solid oxide fuel cells. *J Power Sources* 195:685–702
- Zhao Y, Xia C, Jia L, Wang Z, Li H, Yu J, Li Y (2013) Recent progress on solid oxide fuel cell: lowering temperature and utilizing non-hydrogen fuels. *Int J Hydrog Energy* 38(36):16498–16517
- Ivers-Tiffée E, Weber A, Herbrist D (2001) Materials and technologies for SOFC-components. *J Eur Ceram Soc* 21:1805–1811
- Tsipis EV, Kharton VV (2008) Electrode materials and reaction mechanisms in solid oxide fuel cells: a brief review. I. Performance-determining factors. *J Solid State Electrochem* 12:1039–1060
- Xi X, Kondo A, Kozawa T, Naito M (2016) LSCF–GDC composite particles for solid oxide fuel cells cathodes prepared by facile mechanical method. *Adv Powder Technol* 27:646–651
- Tsipis EV, Kharton VV (2008) Electrode materials and reaction mechanisms in solid oxide fuel cells: a brief review. II. Electrochemical behavior vs. materials science aspects. *J Solid State Electrochem* 12:1367–1391
- Tsipis EV, Kharton VV (2011) Electrode materials and reaction mechanisms in solid oxide fuel cells: a brief review. III. Recent trends and selected methodological aspects. *J Solid State Electrochem* 15:1007–1040
- Adler SB (2004) Factors governing oxygen reduction reaction in solid oxide fuel cell cathodes. *Chem Rev* 104:4791–4843
- Setevich CF, Moggi LV, Caneiro A, Prado FD (2012) Optimum cathode configuration for IT-SOFC using  $\text{La}_{0.4}\text{Ba}_{0.6}\text{CoO}_{3-\delta}$  and  $\text{Ce}_{0.9}\text{Gd}_{0.1}\text{O}_{1.95}$ . *Int J Hydrog Energy* 37:4895–4901
- McCoppin J, Young D, Reitz T, Maleszewski A, Mukhopadhyay S (2011) Solid oxide fuel cell with compositionally graded cathode functional layer deposited by pressure assisted dual-suspension spraying. *J Power Sources* 196:3761–3765
- Huang B, Zhu X, Nie H, Niu Y, Li Y, Cheng N (2013) Comparison of the electrochemical properties of impregnated and functionally gradient  $\text{LaNi}_{0.6}\text{Fe}_{0.4}\text{O}_{3-\delta}$ - $\text{Gd}_{0.2}\text{Ce}_{0.8}\text{O}_2$  composite cathodes for solid oxide fuel cell. *J Power Sources* 235:20–28
- Haanappel VAC, Jordan N, Mai A, Mertens J, Serra JM, Tietz F, et al. (2009) Advances in research, development, and testing of single cells at forschungszentrum jülich. *J Fuel Cell Sci Technol* 6:021302
- Tanner CW, Fung KZ, Virkar AV (1997) The effect of porous composite electrode structure on solid oxide fuel cell performance. *J Electrochem Soc* 144(1):21–30
- Rieu M, Sayers R, Laguna-Bercero MA, Skinner SJ, Lenormand P, Ansart F (2010) Investigation of graded  $\text{La}_2\text{NiO}_{4+\delta}$  cathodes to improve SOFC electrochemical performance. *J Electrochem Soc* 157(4):B477–B480
- Woolley RJ, Skinner SJ (2014) Functionally graded composite  $\text{LaNiO}$  and  $\text{LaNiO}$  solid oxide fuel cell cathodes. *Solid State Ionics* 255:1–5
- Hildenbrand N, Boukamp B, Nammensma P, Blank D (2011) Improved cathode/electrolyte interface of SOFC. *Solid State Ionics* 192:12–15
- Hildenbrand N, Nammensma P, Blank DHA, Bouwmeester HJM, Boukamp BA (2013) Influence of configuration and microstructure on performance of  $\text{La}_2\text{NiO}_{4+\delta}$  IT-SOFC cathodes. *J Power Sources* 238:442–453
- Dumaisnil K, Fasquelle D, Mascot M, Rolle A, Roussel P, Minaud S, et al. (2014) Synthesis and characterization of  $\text{La}_{0.6}\text{Sr}_{0.4}\text{Co}_{0.8}\text{Fe}_{0.2}\text{O}_3$  films for solid oxide fuel cell cathodes. *Thin Solid Films* 553:89–92
- Hwang HJ, Moon JW, Lee S, Lee EA (2005) Electrochemical performance of LSCF-based composite cathodes for intermediate temperature SOFCs. *J Power Sources* 145:243–248
- Mineshige A, Izutsu J, Nakamura M, Nigaki K, Abe J, Kobune M (2005) Introduction of A-site deficiency into  $\text{La}_{0.6}\text{Sr}_{0.4}\text{Co}_{0.2}\text{Fe}_{0.8}\text{O}_{3-\delta}$  and its effect on structure and conductivity. *Solid State Ionics* 176:1145–1149
- Tai LW, Nasrallah MM, Anderson HU, Sparlin DM, Sehlin SR (1995) Structure and electrical properties of  $\text{La}_{1-x}\text{Sr}_x\text{Co}_{1-y}\text{Fe}_y\text{O}_{3-\delta}$  part 2. The system  $\text{La}_{1-x}\text{Sr}_x\text{Co}_{0.2}\text{Fe}_{0.8}\text{O}_{3-\delta}$ . *Solid State Ionics* 76:273–283
- Tu HY, Takeda Y, Imanishi N, Yamamoto O (1999)  $\text{Ln}_{0.4}\text{Sr}_{0.6}\text{Co}_{0.8}\text{Fe}_{0.2}\text{O}_{3-\delta}$  ( $\text{Ln} = \text{La, Pr, Nd, Sm, Gd}$ ) for the electrode in solid oxide fuel cells. *Solid State Ionics* 117:277–281
- Skinner SJ, Kilner JA (2003) Oxygen ion conductors. *Mater Today* 6:30–37
- Baon F, Jiabao Y, Xiaochao Y (2011) The ionic conductivity, thermal expansion behavior, and chemical compatibility of  $\text{La}_{0.54}\text{Sr}_{0.44}\text{Co}_{0.2}\text{Fe}_{0.8}\text{O}_{3-\delta}$  as SOFC cathode material. *Solid State Sci* 13:1835–1839
- Chiba R, Tabata Y, Komatsu T, Orui H, Nozawa K, Arakawa M, et al. (2008) Property change of a  $\text{LaNi}_{0.6}\text{Fe}_{0.4}\text{O}_3$  cathode in the initial current loading process and the influence of a ceria interlayer. *Solid State Ionics* 178(31–32):1701–1709
- Dissertações e teses by autor (2014), Minas Gerais, Brazil <http://www.bibliotecadigital.ufmg.br/dspace/handle/1843/SFSA-9M4N6G>
- Santos JAF, Kleitz M, Matencio T, Domingues RZ (2012) Evaluation of the electrode/electrolyte contact quality in solid oxide fuel cells. *Electrochim Acta* 60:224–229
- Fu CJ, Liu QL, Chan SH, Ge XM, Pasciak G (2010) Effects of transition metal oxides on the densification of thin-film GDC electrolyte and on the performance of intermediate-temperature SOFC. *Int J Hydrog Energy* 35:11200–11207
- Ullmann H, Trofimenko N, Tietz F, Stöver D, Ahmad-Khanlou A (2000) Correlation between thermal expansion and oxide ion transport in mixed conducting perovskite-type oxides for SOFC cathodes. *Solid State Ionics* 138(1–2):79–90
- Kuhna M, Hashimoto S, Sato K, Yashiro K, Mizusaki J (2013) Thermo-chemical lattice expansion in  $\text{La}_{0.6}\text{Sr}_{0.4}\text{Co}_{1-y}\text{Fe}_y\text{O}_{3-\delta}$ . *Solid State Ionics* 241:12–16
- Jiang T, Wang Z, Ren B, Qiao J, Sun W, Sun K (2014) Compositionally continuously graded cathode layers of  $(\text{Ba}_{0.5}\text{Sr}_{0.5})(\text{Fe}_{0.91}\text{Al}_{0.09})\text{O}_3$  and of  $\text{Gd}_{0.1}\text{Ce}_{0.9}\text{O}_2$  by wet powder spraying technique for solid oxide fuel cells. *J Power Sources* 247:858–864
- Kim J, Kim G, Moon J, Park Y, Lee W, Kobayashi K, Nagai M, Kim C (2001) Characterization of LSM-YSZ composite electrode by ac impedance spectroscopy. *Solid State Ionics* 143:379–389
- Barbucci A, Carpanese P, Cerisola G, Viviani M (2005) Electrochemical investigation of mixed ionic/electronic cathodes for SOFCs. *Solid State Ionics* 176:1753–1758
- Garcia EM, Tarôco HA, Matencio T, Domingues RZ, dos Santos JAF (2012) Electrochemical study of  $\text{La}_{0.6}\text{Sr}_{0.4}\text{Co}_{0.8}\text{Fe}_{0.2}\text{O}_3$  during oxygen evolution reaction. *Int J Hydrog Energy* 37:6400–6406